Journal Pre-proofs

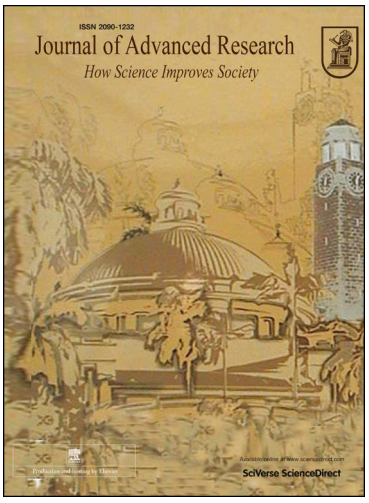

TRPM2-mediated feed-forward loop promotes chondrocyte damage in osteoarthritis via calcium-cGAS-STING-NF-κB pathway

Kai Sun, Xiong Zhang, Liangcai Hou, Fan Lu, Haigang Liu, Zehang Zheng, Zhou Guo, Jingting Xu, Zhaoxuan Ruan, Yanjun Hou, Junchen He, Fengjing Guo, Kaixiang Yang

PII: S2090-1232(24)00499-5
DOI: https://doi.org/10.1016/j.jare.2024.11.007
Reference: JARE 1880

To appear in: *Journal of Advanced Research*

Received Date: 2 May 2024
Revised Date: 2 November 2024
Accepted Date: 3 November 2024

Please cite this article as: Sun, K., Zhang, X., Hou, L., Lu, F., Liu, H., Zheng, Z., Guo, Z., Xu, J., Ruan, Z., Hou, Y., He, J., Guo, F., Yang, K., TRPM2-mediated feed-forward loop promotes chondrocyte damage in osteoarthritis via calcium-cGAS-STING-NF-κB pathway, *Journal of Advanced Research* (2024), doi: https://doi.org/10.1016/j.jare.2024.11.007

Title page

Original article

TRPM2-mediated feed-forward loop promotes chondrocyte damage in osteoarthritis via calcium-cGAS-STING-NF-κB pathway

Kai Sun[a, #], Xiong Zhang[a, #], Liangcai Hou[a], Fan Lu[a], Haigang Liu[a], Zehang Zheng[a], Zhou Guo[a], Jingting Xu[a], Zhaoxuan Ruan[a], Yanjun Hou[a], Junchen He[a], Fengjing Guo[a, *], Kaixiang Yang [b, *]

[a]Department of Orthopedics, Tongji Hospital, Tongji Medical College, Huazhong University of Science and Technology, Wuhan, Hubei 430030, China.

[b]Department of Orthopedic Surgery, Wuhan Fourth Hospital, Puai Hospital, Tongji Medical College, Huazhong University of Science and Technology, Wuhan 430033, China.

*Corresponding authors:

Fengjing Guo, Department of Orthopedics, Tongji Hospital, Tongji Medical College, Huazhong University of Science and Technology, Wuhan, Hubei 430030, China.

Tel./ Mobile Number: +86-27-8366 5238; Fax: +86-27-8366-3670

E-mail: guofjdoc@163.com

Kaixiang Yang, Department of orthopedic Surgery, Wuhan Fourth Hospital, Wuhan 430033, China. Tel./ Mobile Number: +86-27-8366 5218; Fax: +86-27-8366-3540

Email: yangkxdr@126.com

Kai Sun[#] and Xiong Zhang[#] contributed equally to this work.

Credit author statement

KS, FJG, and KXY conceived and designed the study. KS, XZ, LCH, FL, HGL, ZHZ and JTX performed the experiments. ZG and YJH performed a statistical analysis. KS and XZ wrote the manuscript. ZXR and JCH drew revised the manuscript. FJG and KXY acquired funding, reviewed and edited the manuscript. All authors have read and approved the final version of the manuscript.

Kai Sun[#] and Xiong Zhang[#] contributed equally to this work.

Conflicts of interest

The authors declare no conflicts of interest.

Research Highlights

- TRPM2 was highly expressed in cartilage of patients with OA, post-traumatic OA mice, and inflammatory chondrocytes.
- TRPM2 was essential for chondrocyte damage and murine OA progression.
- TRPM2 expression was upregulated in an NF-κB-p65-dependent manner.
- TRPM2 mediated pathologic feed-forward loop in chondrocytes via the Ca2+-cGAS-STING-NF-κB axis.
- Inhibition of TRPM2-Ca^{2+} axis with BAPTA-AM protected against post-traumatic OA in mice.

This study may provide new insights into understanding the pathogenesis of OA in term of TRPM2 mediated feed-forward loop in chondrocytes and suggest that TRPM2-Ca2+ axis may be a novel therapeutic target for OA.

Graphical abstract

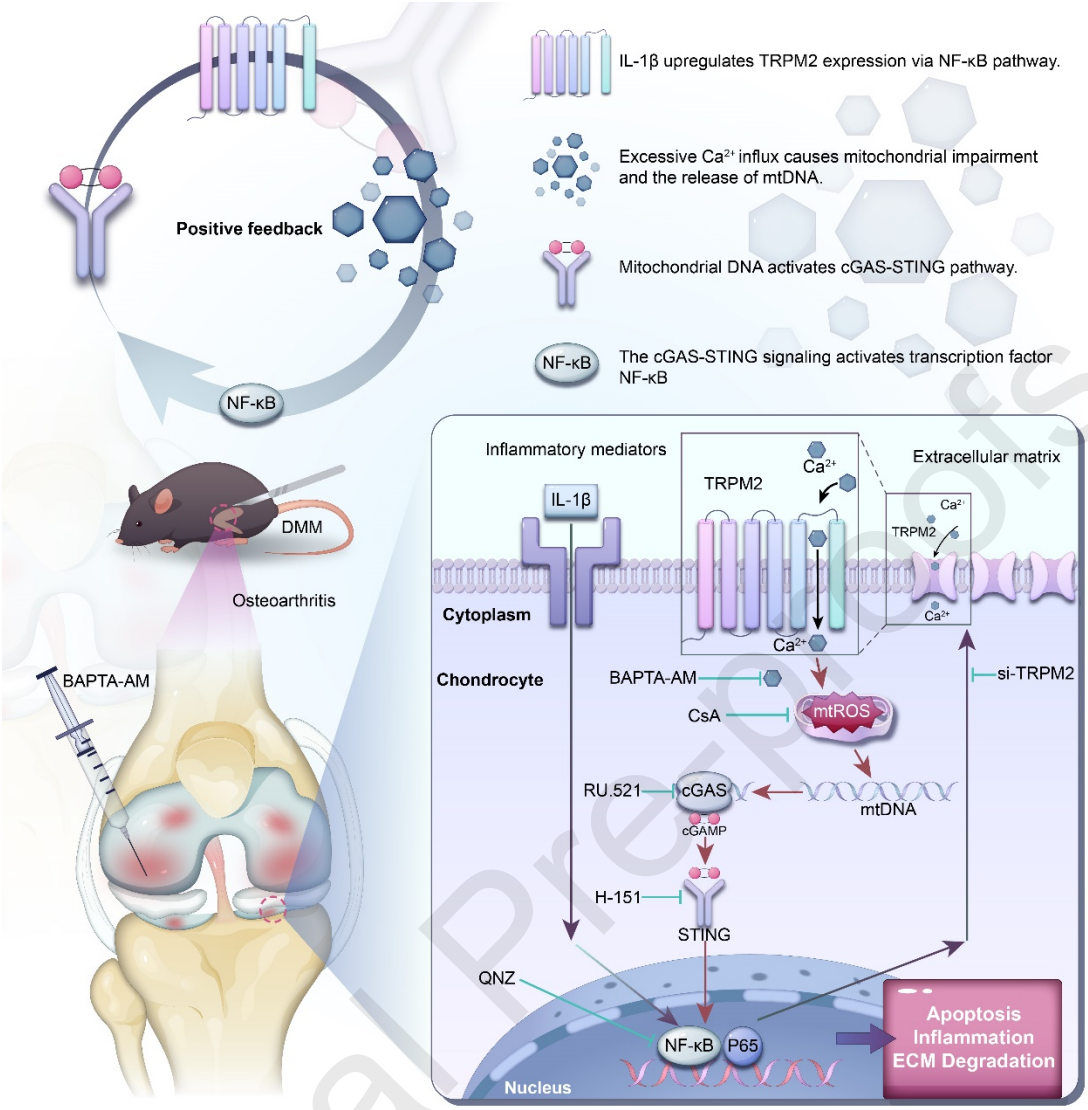

• TRPM2-mediated feed-forward loop promotes chondrocyte damage in osteoarthritis via calcium-cGAS-STING-NF-κB pathway

• Inhibiting TRPM2-Ca^{2+} axis with BAPTA-AM may be a novel strategy for OA treatment.

Compliance with Ethics Requirements

The collection of human cartilage was approved by the Ethics Committee of Tongji Hospital (TJ-IRB20210905) after obtaining informed consent from the patients. The animal experiment was approved by the Ethics Committee of Tongji Hospital (TJH-202212051).

Declarations of interest: none

Manuscript

Original article

TRPM2-mediated feed-forward loop promotes chondrocyte damage in osteoarthritis via calcium-cGAS-STING-NF-κB pathway.

Abstract

Introductions: Osteoarthritis (OA) is a significant contributor to disability in the elderly population. However, current therapeutic options are limited. The transient receptor potential melastatin 2 (TRPM2) is involved in a range of disease processes, yet its role in OA remains unclear.

Objectives: To investigate the role of TRPM2 in OA.

Methods: Cartilage samples were collected from patients with osteoarthritis (OA) and mice with OA to examine TRPM2 expression levels. To investigate the effects of TRPM2 modulation on the destabilization of the medial meniscus (DMM) induced knee OA in mice, we utilized TRPM2 knockout mice and employed adenovirus-mediated overexpression of TRPM2. Furthermore, siRNA-mediated TRPM2 knockdown or plasmid-mediated TRPM2 overexpression was conducted to explore the role of TRPM2 in IL-1β-induced chondrocytes. The regulatory mechanism of IL-1β on TRPM2 expression was screened by signaling pathway inhibitors, and the transcription factors and binding sites of TRPM2 were predicted using the database. The binding of RELA (NF-κB-p65) to the Trpm2 promoter was verified by chip-PCR and ChIP-qPCR. The therapeutic potential of Ca^{2+} chelation with BAPTA-AM for the treatment of osteoarthritis (OA) was investigated.

Results: An increased expression of TRPM2 was observed in the cartilage of OA patients and OA mice. Furthermore, mice deficient in Trpm2 exhibited a protective effect against DMM-induced OA progression. In contrast, TRPM2 overexpression resulted in exacerbation of DMM-induced OA and the promotion of an OA-like phenotype of chondrocytes. TRPM2 was upregulated by IL-1β in an NF-κB-p65-dependent manner. Subsequently, the TRPM2-Ca^{2+}-mtDNA-cGAS-STING-NF-κB axis in the progression of OA was validated. Furthermore, inhibition of the TRPM2-Ca^{2+} axis with BAPTA-AM effectively attenuated established OA.

Conclusions: Our data collectively revealed a pathological feedback loop involving TRPM2, Ca^{2+}, mtDNA, cGAS, STING, and NF-κB in OA chondrocytes. This suggests that disrupting this loop could be a viable therapeutic approach for OA**.**

KEY WORDS: osteoarthritis; chondrocyte; TRPM2; calcium ions; NF-κB

Abbreviations:

OA: osteoarthritis; TRPM2: transient receptor potential melastatin 2; OARSI: Osteoarthritis Research Society International; IL-1β: interleukin-1β; DMM: destabilization of the medial meniscus; PFUs: plaque-forming units; IF: immunofluorescence; ADAMTS5: ADAM metallopeptidase with thrombospondin type 1 motif 5; AdV: Adenoviruses; Ca^{2+}: Calcium ion; $CaCl_2$: calcium chloride; CCK8: Cell counting kit-8; cGAS: Cyclic GMP-AMP Synthase; COL2A1: collagen type II alpha 1 chain; CsA: Cyclosporin A; ECM: extracellular matrix; EdU: Ethynyl-2′-deoxyuridine; H&E: hematoxylin-eosin; NF-κB: Nuclear factor kappa B; IHC: immunohistochemistry; KEGG: Kyoto encyclopedia of genes and genomes; siRNA: small interfering RNA; STING: stimulator of interferon genes; micro-CT: Micro-computed tomography; MMP13: matrix metallopeptidase 13; ChIP: chromatin immunoprecipitation; MMP3: matrix metallopeptidase 3; mtDNA: mitochondrial DNA; NAC: N-Acetyl-l-cysteine; NC: Negative control; RNA-seq: RNA sequencing; iNOS: inducible nitric oxide synthase; TFs: transcription factors; WT: wild type; COX2: cyclooxygenase-2; Cytochrome c: Cyt C; BCL2-Associated X: Bax; B-cell lymphoma-2: Bcl2;D-Loop2: Displacement loop 2; D-Loop3: Displacement loop3.

Introduction

Osteoarthritis (OA) is one of the most prevalent degenerative joint diseases[1]. The precise molecular mechanism underlying OA pathogenesis remains largely unknown[1]. Chondrocytes play a pivotal role in maintaining cartilage homeostasis and integrity[2]. Damage and dysfunction of chondrocytes contribute to the initiation and progression of OA[3]. Conducting in-depth research on the molecular mechanisms underlying chondrocyte damage is essential for developing targeted therapeutic approaches.

Calcium ions (Ca^{2+}) have a role in cell signaling, hormone regulation, and cell growth[4]. Loss of Ca^{2+} homeostatic control, which can result from excessive channel stimulation or cytosolic leakage, is a significant contributor to cell death[5]. The cytosolic overload of Ca^{2+} triggers mitochondrial permeability transition and cytochrome c release into the cytosol, ultimately activating caspases and promoting apoptosis[6]. Previous studies have demonstrated that excess cytosolic Ca^{2+} contributes to chondrocyte damage and the development of osteoarthritis (OA)[7,8]. Therefore, it is evident that the precise regulation of Ca^{2+} concentration in the chondrocyte is required for the prevention or protection against OA.

Transient receptor potential melastatin 2 (TRPM2) is a non-selective Ca^{2+}-permeable cation channel that is gated by intracellular ADP-ribose (ADPR) [9,10]. It is highly sensitive to activate by oxidative stress-inducing stimuli[9]. Many studies have demonstrated that the TRPM2 channel mediates intracellular Ca^{2+} homeostasis and oxidative stress, suggesting its significant contribution to degenerative diseases[11-13]. Given the association between oxidative stress and Ca^{2+} homeostasis with the progression of OA[7,14], it can be postulated that TRPM2 may play a role in this disease.

The study aims to investigate the potential role of TRPM2 in the pathogenesis of osteoarthritis (OA). Our findings suggest that TRPM2 contributes to OA pathogenesis through a Ca^{2+}-associated pathway and that targeting the TRPM2-Ca^{2+} axis may be an effective OA therapy. To this end, we observed the TRPM2 expression in cartilage and chondrocytes. Furthermore, we investigated the role of TRPM2 in OA using Trpm2 knockout mice and adenovirus tools. Moreover, we sought to elucidate the pathogenic mechanism of TRPM2 and explore the potential therapeutic benefits of Ca^{2+} chelation for treating OA.

Materials and methods

Mouse chondrocyte

Primary chondrocytes were isolated from wild-type (WT) and *Trpm2*-KO C57BL/6J mice (5-day-old). The cartilage of the knee joint was removed and ground. Next, trypsin was used to digest the cartilage pieces for 30 minutes. After trypsin removal, type 2 collagenase (0.25%) was used to digest the cartilage tissues for 6h. Subsequently, the type 2 collagenase was removed and the resuspended chondrocytes were cultured in a chondrogenic medium (DMEM/F12 medium with 1% streptomycin sulfate, 1% penicillin, and 10% FBS). The cells were maintained in an incubator under stable conditions and appropriate humidity. The first- and second-generation chondrocytes were utilized in our experiments.

Human cartilage samples

The OA group samples were collected from 12 OA patients following total knee arthroplasty. The control group samples were collected from 4 amputees (non-OA patients) and the unloading zone of 3 patients with slight knee OA (see Supplementary Table 1-2). Before participation, all patients provided informed consent. The Ethics Committee of Tongji Hospital approved the study (Ethics approval number: TJ-IRB20210905).

Materials and reagents

Selleck Chemicals provided the following compounds: BAPTA-AM (S7534), RU521 (S6841), Cyclosporine A (S1514), H-151 (S6652), SP600125 (S1460), and LY294002 (S1105). DMSO (HY-Y0320) and QNZ (HY-13812) were procured from Med Chem Express (MCE, USA). Mouse IL-1β was sourced from R&D Systems (401-ML-010/CF, USA). $CaCl_2$ (C4901) was obtained from the Solarbio Company (Beijing, China). Fetal bovine serum (FBS-NZ500) was procured from NEWZERUM (New Zealand). The trypsin, type 2 collagenase, streptomycin sulfate, penicillin, and DMEM/F12 medium were sourced from BOSTER Biological Technology (Wuhan, China).

Ethynyl-2'-deoxyuridine (EdU) staining.

An EdU staining kit (Ribobio, China) was utilized to assess the impact of BAPTA-AM at varying concentrations on the proliferation of chondrocytes. Initially, chondrocytes were incubated with the EdU medium to incorporate EdU into the DNA. Subsequently, the chondrocytes were fixed with paraformaldehyde for 30 minutes. Then, the 1×Apollo staining reaction solution was added and incubated for 30 minutes in a decolorizing shaker. Finally, the chondrocytes were stained with a solution of Hoechst. The images were obtained using a fluorescence microscope (Evosfl Auto, USA).

Cell counting kit-8 (CCK8) assay

The viability of chondrocytes was evaluated using a CCK-8 kit (Med Chem Express, HY-K0301). Chondrocytes were treated with varying concentrations of BAPTA-AM. Following treatment, the old media was removed and serum-free media containing CCK-8 solution was added, and the cells were incubated in the dark for 1 h. The absorbance was then measured at 450 nm.

TRPM2 knockdown and overexpression in chondrocytes

Tsingke Biotech (Wuhan, China) provided qualified si-*Trpm2* and negative control siRNA. The sequence used in our experiment was as follows: si-*Trpm2* 1# CCAAGAUAAUCAUCGUGAATT; si-*Trpm2* 2#: GCACUCUGCAUACAAUCUAT T; si-*Trpm2* 3#: GGAUUCCCGAGAAUAUCAATT. Chondrocytes were cultured and transfected when they reached an appropriate density with 20 nmol siRNA using Lipo3000 (Invitrogen, L3000015). AuGCT DNA-SYN Biotechnology (Wuhan, China) provided us with the qualified plasmid of Trpm2 and the negative control plasmid. Chondrocytes were transfected with plasmid and Lipo3000 and P3000TM reagent (Invitrogen, L3000015).

Intracellular Ca^{2+} imaging

Fluo-4 AM (Beyotime Biotechnology, China) was utilized to quantify intracellular calcium levels. Following the administration of the treatment, the media was removed and the cells were washed with HBSS. HBSS-diluted Fluo-4 AM working fluid (2 μM) was added and incubated at 37°C for 1 h. The cells were then washed with HBSS and incubated with HBSS for 20 min. Finally, the images were obtained using a fluorescence microscope (Evosfl auto, USA).

Detection of mtDNA in the cytosol

The mtDNA release assay was conducted following the previously described methodology[15,16]. Chondrocytes were uniformly cultured (cell counting-based) in six culture dishes and randomly allocated to three groups: Ctrl, IL-1β, and $CaCl_2$ group, with two culture dishes in each group. Total DNA was extracted from the cells of one cell dish from each group. Pure cytoplasmic components were obtained from the other

cell dish. Subsequently, a QIAQuick Nucleotide Removal Column was employed to obtain the DNA present in the cytoplasmic components. Quantitative PCR was utilized to determine the nuclear DNA (Tert) and mitochondrial DNA (D-Loop2 and D-Loop3) present in the total DNA and cytoplasmic DNA. The primer sequences are as follows: Tert: F:5'-CTAGCTCATGTGTCAAGACCCTCTT-3', (R): 5'-GCCAGCACGTTTCTCTCGTT-3'; D-loop2: (F): 5'-CCCTTCCCCATTTGGTCT-3', R: 5'-TGGTTTCACGGAGGATGG-3'; D-loop3: (F): 5'-TCCTCCGTGAAACCAACAA-3', (R): AGCGAGAAGAGGGGCATT-3'. The Ct value for mtDNA abundance in the total DNA was employed as a normalization control for comparing the changes in mtDNA levels in the cytoplasmic components.

JC-1 potentiometric staining

The mitochondrial membrane potential in chondrocytes was assessed using the JC-1 dye (Beyotime, China). The chondrocytes were treated with si-NC or si-*Trpm2* for 48 hours, followed by the induction with IL-1β for 12 hours. Then, 500 μl of the JC-1 dye working solution (5 μM) was added to each well of the 12-well plate and incubated for 30 minutes. The images were obtained using a fluorescence microscope (Evosfl Auto, USA).

Mitochondrial ROS Detection

A Mito Sox Red assay kit from (Yeason, China), was employed to quantify the mitochondrial ROS level in chondrocytes. In brief, chondrocytes were treated with si-NC or si-*Trpm2* for 48 hours, followed by the induction with IL-1β for 12 hours. After the treatment, cells were stained with the Mito Sox Red probe (5 μM) for 30 minutes. Subsequently, the chondrocytes were washed with preheated HBSS three times. The images were obtained using a fluorescence microscope (Evosfl Auto, USA).

In vitro Toluidine blue and Safranin O staining

Toluidine blue staining and Safranin O staining were employed to observe the morphology of chondrocytes. In brief, chondrocytes were treated with IL-1β, CaCl2, and BAPTA-AM. Following treatment, chondrocytes were fixed with paraformaldehyde, and then the toluidine blue (Servicebio, Wuhan, China) or Safranin O solution (Servicebio, Wuhan) was added and allowed to incubate for one hour. Subsequently, the cells were washed and images were obtained using a microscope (Evosfl auto, Life Technologies, USA).

In vivo overexpression of TRPM2 using Adenovirus

The adenoviral vectors carrying GFP and TRPM2 were designed by Vigene Biosciences (Shandong, China). One week after the adaptive feeding in the animal biosafety laboratory level 2 (ABSL-2) located within the Experimental Animal Center

of Tongji Hospital, the mice underwent a DMM surgery or a sham operation. After a week, 10 μl of Ad-TRPM2 (1 × 109 PFUs) or Ad-negative adenoviruses (1 × 109 PFUs) were injected intra-articularly once weekly for 8 weeks[17]. The knee joints were collected for histological analyses after administering either Ad-TRPM2 or Ad-negative adenoviruses for eight weeks.

Animal experiment

All animal experiment procedures were approved by the Ethics Committee of Tongji Hospital (TJH-202212051). The wild-type (*Trpm2*+/+, C57BL/6 background) and Trpm2 knockout mice (*Trpm2*−/−, C57BL/6 background) were generated by Cyagen Biosciences (Suzhou, China). The depletion of *Trpm2* was confirmed by DNA genotyping using a standard polymerase chain reaction (PCR) assay (supplementary Fig.1). Genotyping of *Trpm2*−/− mice was performed using the following primers: primers1:(F):5'-TTGGTTAGGTGGTCCATTCATGC-3', (R):5'-TGGTAAAATGAGCTTCATACCTCC -3', and primers2:(F):5'-AAAGAATCAGGGAACCAGGAGTAA-3', (R):5'-TGGTA AAATGAGCTTCATACCTCC-3'. The sham operation or DMM model was established in adult male *Trpm2*-KO and WT mice. Eight weeks after the DMM surgery, the OA phenotype was compared between four groups (Sham-WT, *Trpm2*-KO, WT + DMM, *Trpm2*-KO + DMM). To investigate the effect of overexpression of TRPM2 in vivo, fifty 8-week-old WT mice were divided into five groups: The groups were designated as follows: Sham + AdV-GFP, Sham + AdV-TRPM2, DMM + AdV-GFP, DMM + AdV-TRPM2, and DMM + AdV-TRPM2 + BAPTA-AM. To investigate the in vivo therapeutic effect of BAPTA-AM, WT mice were divided into three groups: The experimental groups were designated as follows: DMM, DMM + BAPTA-AM (1.5 μg/kg), and DMM + BAPTA-AM (15 μg/kg). A total of 10 μl BAPTA-AM or vehicle solution was injected into the right knee joint once per week for 8 weeks. Following this period, the knee joints were collected for histological analysis.

Western blot analysis

The 10% or 12.5% SDS-PAGE gels (Epizyme Biotech, PG112, PG213) were employed to separate the chondrocyte total protein samples. The separated protein samples on the gels were transferred to polyvinyl difluoride membranes (Millipore, USA). Subsequently, the membranes were incubated in a blocking solution (Boster, AR0041) for 20 minutes, after which they were probed with a series of antibodies. These included TRPM2 (Novus Biologicals, NB110-81601; diluted at 1:1500), COL2A1 (CST, #43306; dilution 1:1500), SOX9 (ab185966, Abcam, dilution 1:5000), P53 (Proteintech, 60283-2-Ig, dilution 1:1500), COX2 (Abcam, ab179800, 1:1500), GAPDH (CST, #97166, 1:1500), β-ACTIN (CST, #4970, dilution 1:1500), and MMP3 (CST, #14351; 1:1500), MMP13 (Proteintech, 18165-1-AP, 1:1500), STING (Proteintech, 19851-1-AP, 1:1500), NF-κB p65 (Proteintech, 10745-1-AP), Phospho-NF-κB p65 (Proteintech, 82335-1-RR), IKKa (Abcam, ab3204, 1:1500), and cGAS (Proteintech, 29958-1-AP, 1:1500), Phospho-NF-κB p65 (Proteintech, 82335-1-RR1:1500), IKKa (Abcam, ab3204, 1:1500), and cGAS (Proteintech, 29958-1-AP, 1:1500), ADAMTS5 (Boster, A02802-1,1: 1000), Cleaved-caspase 3 (Proteintech, 25128-1-AP, 1:500), iNOS (CST,

#13120; 1: 1500), Cyt C (CST, #4272, 1:1000), Aggrecan (ABclonal, A8536, 1:1000), Bax (CST, #2772, 1:1000), Bcl2 (CST, #15071, 1:1000), and all samples were incubated overnight at 4°C. Subsequently, the PVDF membranes were incubated with the HRP goat anti-mouse or anti-rabbit IgG secondary antibody (Boster, BA1050, BA1054, 1:5000). The images were visualized using a Bio-Rad scanner (Bio-Rad, Hercules, CA).

RT-qPCR

The total chondrocyte RNA was isolated and reverse-transcribed to cDNA. PCR was performed using cDNA for amplification with the SYBR Green Master Mix. The amplification conditions utilized were those described in a previous article[18]. The sequences of the primers were as follows: *Trpm2* (F) 5′-ACAGCAACCATTCCCACTTCA-3′, (R) 5′- CCCTCCAACACCACGCAGA-3'. *Col2a1* (F) 5′-CTGTGGAGGTCACTGTAGAC T-3′, (R) 5′-GAAGGGGATCTCGGGGTTG-3′, *Gapdh* (F) 5′-AGGTTGTCTCCTG CGACTTCA-3′, (R) 5′- GGGTGGTCCAGGGTTTCTTA-3′. *Cox2* (F) 5′-TTCAACA CACTCTATCACTGGC-3′, (R) 5′-AGAAGCGTTTGCGGTACTCAT-3′, *iNOS* (F) 5′-GTTCTCAGCCCAACAATACAAGA-3′, (R) 5′-GTGGACGGGTCGATGTCAC-3′, *Mmp3,* (F) 5′-ACATGGAGACTTTGTCCCTTTTG-3′, (R) 5′-TTGGCTGAGTGGTA GAGTCCC-3′, *Mmp13* (F) 5′-CTTCTTCTTGTTGAGCTGGACTC-3′, (R) 5′-CTGT GGAGGTCACTGTAGACT-3′, *Aggrecan* (F) 5′-CCTGCTACTTCATCGACCCC-3′, (R) 5′-AGATGCTGTTGACTCGAACCT-3′, Each cDNA sample was repeated at least three times.

Immunofluorescence (IF) staining

Following the completion of the treatment regimen, the chondrocytes were fixed with paraformaldehyde and permeabilized with 0.2% Triton X-100 (BioFroxx, 1139ML100). After that, they were blocked with goat serum albumin (Boster, AR0009). The anti-TRPM2 (Novus Biologicals, NB110-81601, 1:200), anti-COL2A1 (Abcam, ab239074, 1:200), anti-MMP13 (Abcam, ab39012, 1:200), and anti-STING (Abcam, ab239074, 1:200) antibodies were used in this study. Subsequently, the Anti-Rabbit or Anti-Mouse IgG Secondary Antibody (Boster, BA1105, BA1031, 1:250) was employed to incubate the cells. Cell nuclei were stained with DAPI (Boster, AR1177). The images were obtained by fluorescence microscopy.

Chromatin immunoprecipitation (ChIP) assay

In brief, the DNA molecules were extracted from the chondrocytes using the ChIP assay kit under the manufacturer's instructions. The ChIP assay was performed using a ChIP assay kit (Beyotime, P2078, China) as previously described[18]. Then, a DNA purification kit (Beyotime, D0033, China) was used to purify the DNA obtained in the previous step. Subsequently, the samples were incubated overnight with the P65

antibody (Proteinthch, 10745-1-AP) or normal rabbit IgG antibody on a rotary shaker at 4 ℃. The samples were then washed from the Protein A + G agarose beads and subjected to ChIP-PCR. PCR amplifications were performed as previously described[18]. Primer 1: The forward (F) and reverse (R) primers used for PCR amplification were as follows: F, 5′-ATCTTGGGCA TAATGTCCTT-3′; R, 5′-GAACTATCCATCCATAAAAAT-3′; and F, 5′-TA CTGGTTCTTTCTGTCTCCTCTGT-3′; R, 5′-TACCCTCCTGCTAAAAGTCCCT-3′.

Micro-computed tomography (micro-CT) analysis

A Viva CT 80 scanner (Scanco Medical AG, Switzerland) micro-CT was employed to analyze the paraformaldehyde-fixed knee joints (100 kV, 98 μA, 10.5 μm). The osteophyte size and subchondral bone were analyzed according to the method previously described in a study by the same authors[18]. The images were acquired using the Scanco Medical software.

Histological analyses

Following the sacrifice of the mice, the postoperative knee joints were collected and subjected to fixation, decalcification, and paraffin embedding. Safranin O/Fast green staining (Servicebio, G1053-100ML), immunohistochemical staining (Servicebio, G1312-100T), and hematoxylin-eosin (H&E) (Servicebio, G1076-500ML) were performed. The current study applied the Osteoarthritis Research Society International (OARSI) scoring system to evaluate cartilage degeneration. The OARSI scores were independently performed by two researchers, with the scoring criteria referenced to the previously published study[18]. Osteophyte size was scored according to the previously published study[19]. Synovitis assessment by H&E slides was conducted according to the previously described criteria[20]. Immunohistochemical staining was performed as previously described[21]. The expression of TRPM2, Aggrecan, MMP13, COL2A1, COX2, ADAMTS5, and iNOS, was observed in the cartilage of the knee joint.

RNA-sequencing

For transcriptome RNA-seq analysis, total RNA was isolated from chondrocytes and RNA sequencing was performed by the BGI Genomics Company (Shenzhen, China). Data were analyzed on the Dr. Tom network platform of BGI.

Statistical analysis

The statistical software utilized was GraphPad Prism 8.0. The one-way analysis of variance (ANOVA) followed by Tukey's post hoc test was employed for multiple group comparisons. At the same time, the unpaired two-tailed Student's t-test was utilized to compare continuous data between the two groups. For nonparametric data, the Mann-Whitney U test was employed to assess differences in OARSI grade between two

groups, while the Kruskal-Wallis test followed by Dunn's post hoc test was utilized for multiple group comparisons. Data are presented as the mean ± SEM, and statistical significance was defined as $P < 0.05$.

Results

TRPM2 expression increased in OA

To identify potential pathologic genes involved in OA pathogenesis, RNA sequencing was performed to analyze the transcriptome changes of IL-1β-treated chondrocytes. The volcano plot analysis revealed the differentially expressed genes between the two groups, and the Kyoto Encyclopedia of Genes and Genomes (KEGG) analysis indicated that the "calcium signaling pathway" was enriched (Fig. 1A, B). Furthermore, a heat map analysis of the "calcium signaling pathway" revealed *Trpm2* as a significantly differentially expressed gene between the two groups (Fig. 1C). To validate the relationship between TRPM2 expression and OA, cartilage samples were collected from OA patients and OA mice for examination. As shown in Fig. 1D and G, severe cartilage degeneration and increased TRPM2 expression were observed in OA cartilage. In DMM-induced OA mice (Fig. 1E, F), we also observed an increase in TRPM2-positive chondrocytes compared to the sham group. Furthermore, we detected TRPM2 expression in primary chondrocytes and found that pro-inflammatory factor IL-1β could induce notably increased mRNA and protein levels of TRPM2 (Fig. 1H-J). Additionally, consistent results regarding TRPM2 expression were obtained through immunofluorescence staining (Fig. 1K). These data collectively support the notion that OA features the induction of TRPM2 overexpression.

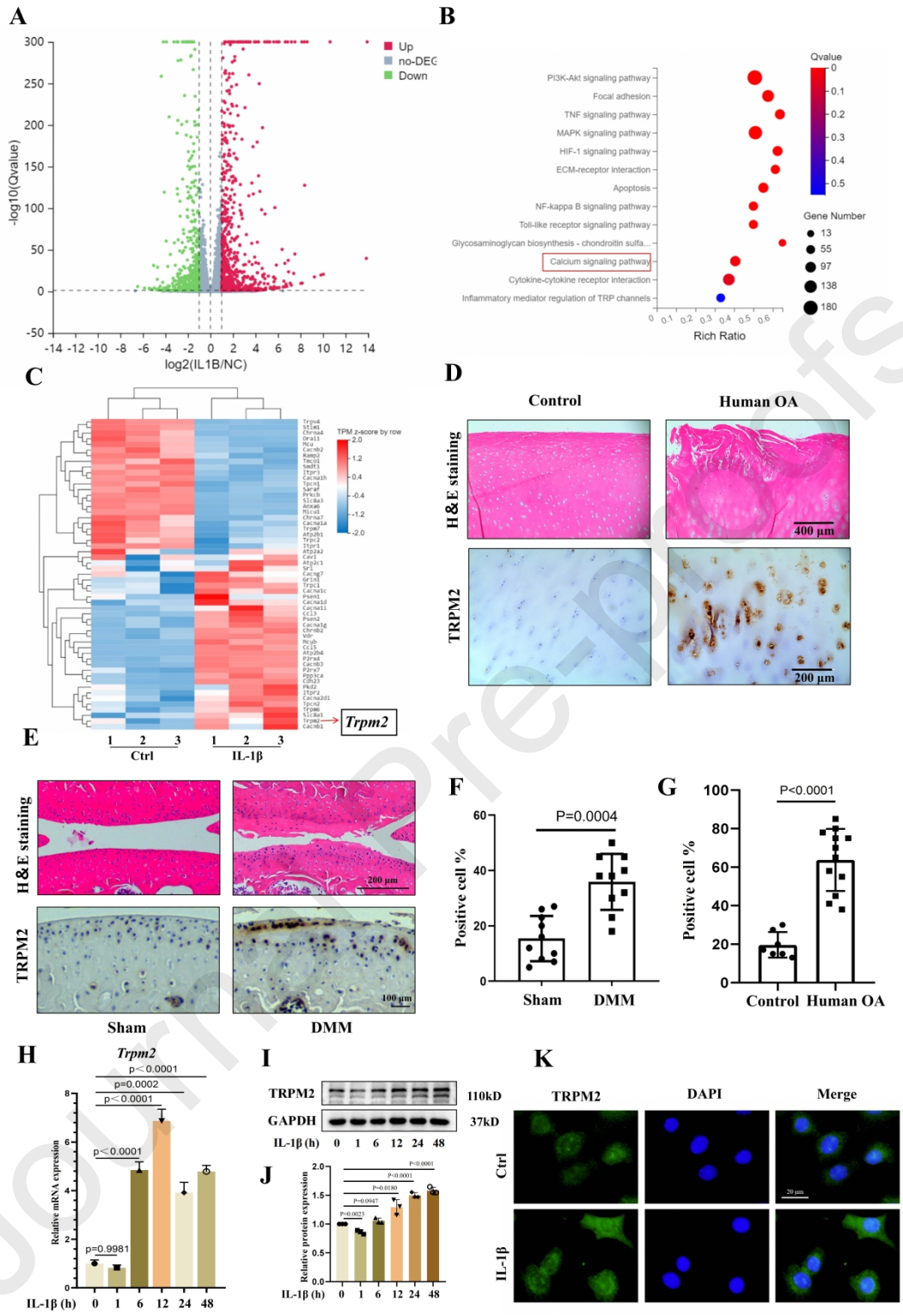

Figure 1 The levels of TRPM2 expression in OA cartilage and chondrocytes were analyzed using RNA sequencing. The volcano plot analysis (A), KEGG analysis (B), and heat map analysis (C) were conducted to compare the Ctrl group and the IL-1β-treated group. The concentration of IL-1β used in this study was 5 ng/ml. (D) H&E and IHC staining of TRPM2 in the cartilage of the OA group and control group (linear scales: 400 μm for H&E staining and 200 μm for IHC staining). (E) H&E and IHC staining of TRPM2 in murine cartilage from the Sham and DMM group (linear scales:

200 μm for H&E staining and 100 μm for IHC staining). (F) Quantitative analysis of TRPM2-positive chondrocytes in murine cartilage (n = 10). (G) Quantitative IHC analysis of TRPM2-positive chondrocytes within the human cartilage (Ctrl, n = 7; OA, n = 12). (H) RT-qPCR analyzed the mRNA levels of *Trpm2* in IL-1β-induced chondrocytes. (I) The TRPM2 expression in IL-1β-induced chondrocytes and (J) statistical protein expression analysis. (K) IF staining results of TRPM2 expression and distribution in IL-1β-induced chondrocytes (linear scale: 20 μm). Data are presented as the mean ± SEM, and p values are from two-tailed unpaired t-tests (F, G, H, J).

Global deletion of Trpm2 alleviates DMM-induced OA

To investigate the role of TRPM2 in OA progression, we subjected *Trpm2*−/− and WT mice to DMM surgery. In contrast to the sham mice, the *Trpm2*-KO mice exhibited resistance to DMM-induced cartilage destruction, as evidenced by reduced proteoglycan loss and cartilage erosion, as well as a lower OARSI score and increased cartilage thickness (Fig. 2A-D). Consequently, the *Trpm2*-KO mice that underwent DMM induction exhibited considerably elevated levels of anabolism (COL2A1 and Aggrecan) (Fig. 2F, J), accompanied by reduced levels of catabolism (MMP13, ADAMTS5) and inflammation (COX2, iNOS) in articular cartilage (Fig. 2F, K).

Osteophyte formation and synovitis are typical pathological features of OA[22,23]. To evaluate the changes in osteophytes and synovium in four groups, we conducted a study. The *Trpm2*-KO mice subjected to DMM surgery exhibited a reduction in osteophyte formation with a minor osteophyte outgrowth (Fig. 2E, H), and exhibited mild inflammation in the synovium, with a lower synovitis score compared to DMM mice (Fig. 2G, I). Collectively, these data indicate that *Trpm2* knockout alleviates DMM-induced OA progression in mice.

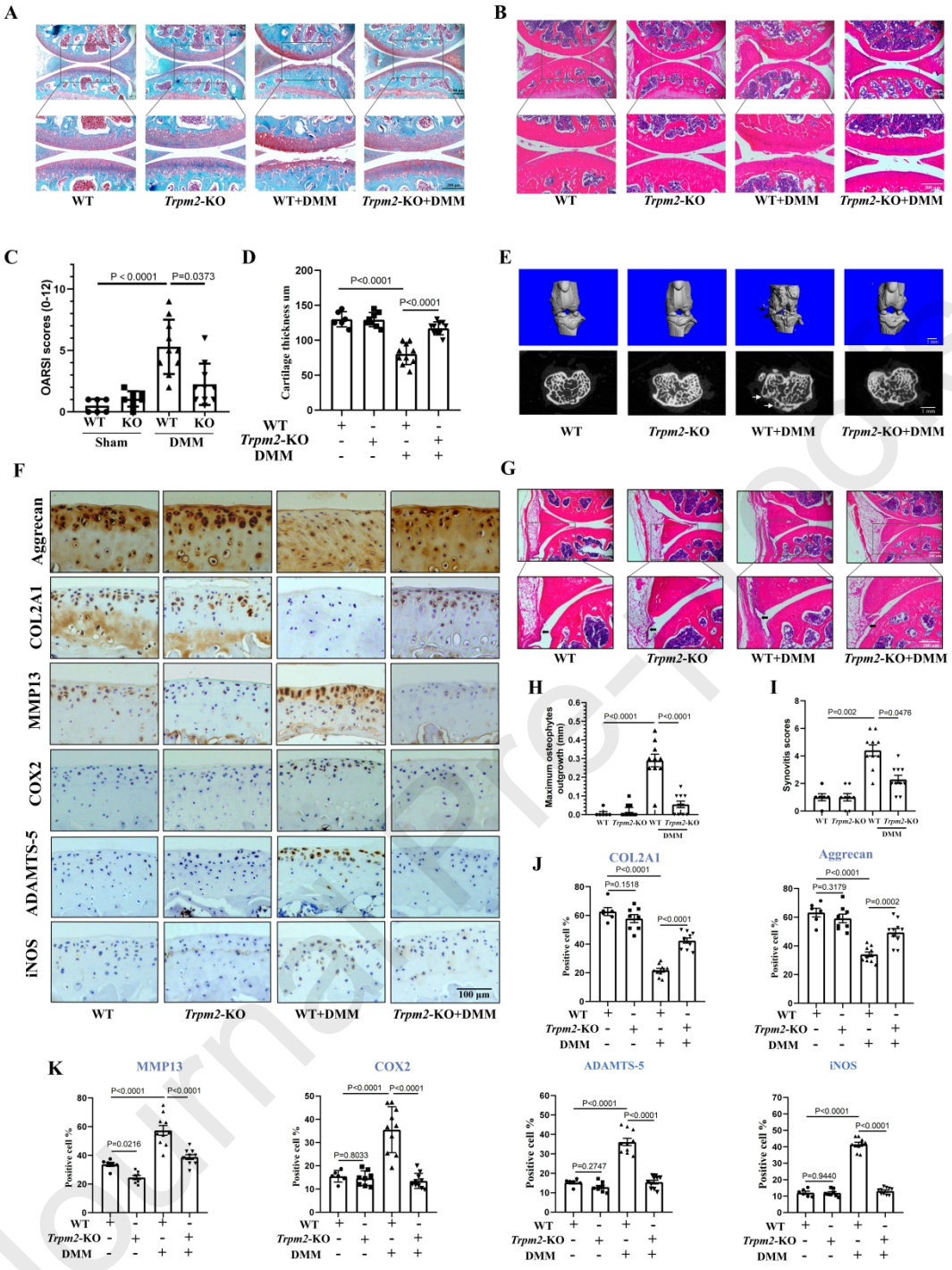

Figure 2 TRPM2 knockout could alleviate DMM-induced OA in mice. (A, B) Safranin O/Fast green staining and H&E results (linear scale = 200 μm). The OARSI analysis (C) and cartilage thickness analysis (D) (Sham group n = 6; *Trpm2*-KO group: n = 8; other two groups: n = 10). (E) 3D reconstruction images and the tibial plateau transverse sectional images, black/white arrow indicates osteophyte (Linear scale = 1 mm). (F) IHC results and (J, K) quantitative analysis of Aggrecan, COL2A1, MMP13, COX2, ADAMTS5, and iNOS (Sham group n = 6; *Trpm2*-KO group: n = 8; other two groups: n = 10; Linear scale = 100 μm). (G) H&E staining for synovium and (I) the quantitative analysis of synovitis scores, the black arrow indicates synovial lining cells (Sham group n = 6; *Trpm2*-KO group: n = 8; other two groups: n = 10; Linear scale = 200 μm). (H)

Quantitation of maximum osteophyte outgrowth (Sham group n = 6; *Trpm2*-KO group: n = 8; other two groups: n = 10; Linear scale = 1 mm). Data are mean ± SEM. p values are from the Kruskal-Wallis test followed by Dunn's post hoc test (C, I), and the one-way ANOVA test followed by Tukey's post hoc test (D, J, K).

TRPM2 overexpression accelerated DMM-induced OA via Ca^{2+}

To further verify the role of TRPM2 in OA, we performed an intra-articular injection of AdV-TRPM2 to overexpress TRPM2 in the cartilage of DMM or sham surgery-induced mice. Immunohistochemistry (IHC) results demonstrated that the number of TRPM2-positive chondrocytes in cartilage was significantly increased in the AdV-TRPM2 group compared to those in the AdV-GFP group (Fig. 3A, B). Notably, TRPM2-overexpressed mice exhibited increased susceptibility to DMM-induced cartilage degeneration, as evidenced by more severe cartilage degeneration and a higher OARSI score (Fig. 3C-E) and decreased cartilage thickness (Supplementary Figure. 1G) when compared to DMM mice. Given that TRPM2 is a non-selective Ca^{2+}-permeable cation channel, we investigated whether the effect of TRPM2 in OA is dependent on Ca^{2+}. An intra-articular injection of the Ca^{2+} chelator BAPTA-AM (15 μg/kg) was administered, and it was found that Ca^{2+} chelation could partially alleviate the exacerbation of cartilage degeneration caused by overexpression of TRPM2 (Fig. 3C-E, Supplementary Figure. 1G). Following the aforementioned observations, the TRPM2-overexpressed mice following DMM induction displayed significantly higher levels of catabolism (MMP13, ADAMTS5) and inflammation (COX2, iNOS), and lower levels of anabolism (COL2A1 and Aggrecan) in cartilage. Conversely, chelation of Ca^{2+} largely reversed these changes (Fig. 3F, G). Furthermore, TRPM2 overexpression markedly accelerated osteophyte formation and synovitis in DMM mice, as evidenced by increased outgrowth of osteophyte and lining cells in the synovium (Fig. 3H-L). Notably, chelation of Ca^{2+} counteracted these effects caused by TRPM2 overexpression. Collectively, our data suggest that TRPM2 overexpression in cartilage exacerbates OA progression in mice, at least partially, via Ca^{2+}.

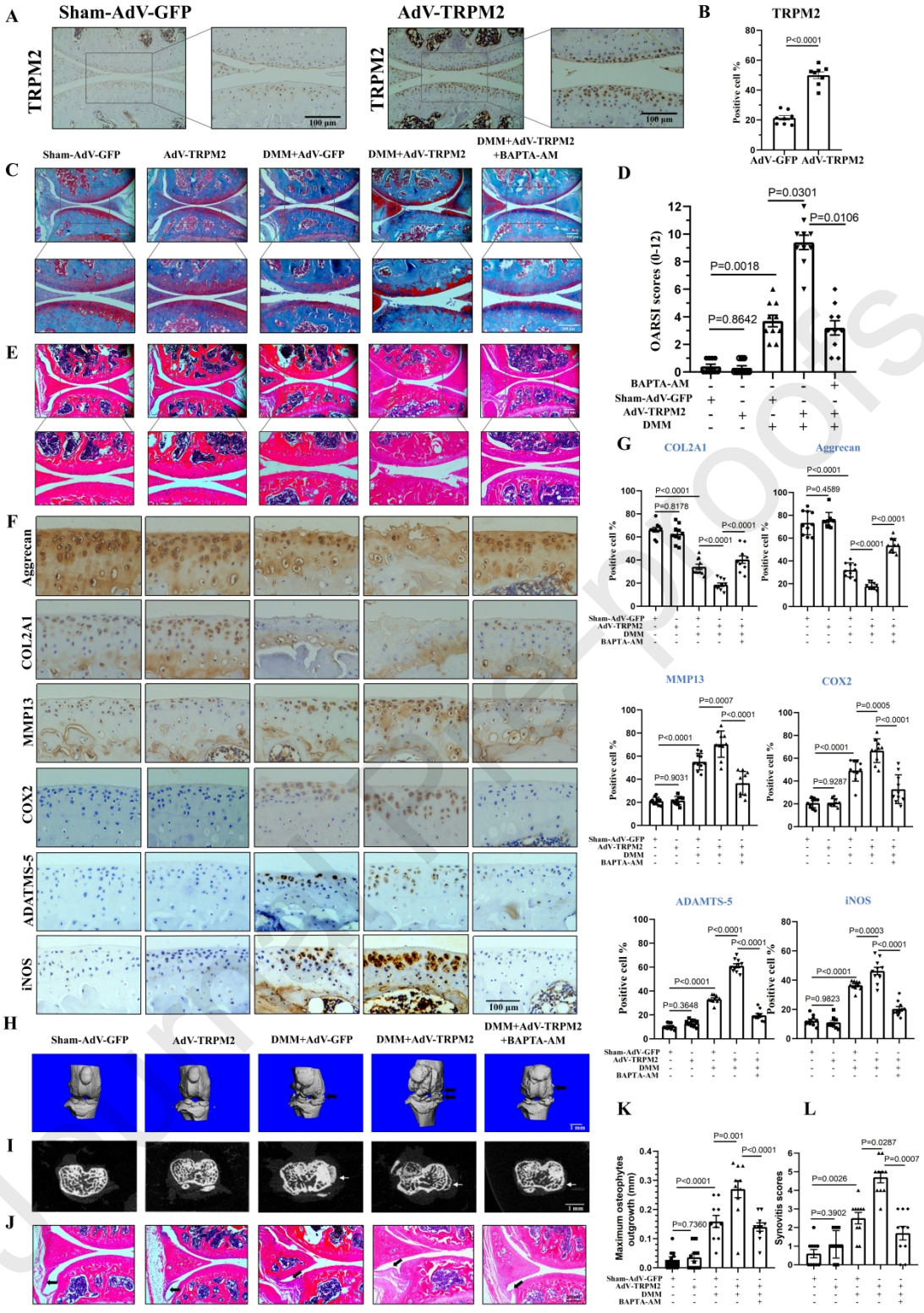

Figure 3 TRPM2 overexpression exacerbated OA phenotype in DMM-induced OA mice. (A) IHC results and (B) quantitative analysis of TRPM2-positive chondrocytes in sham-AdV-GFP and AdV-TRPM2 group mice (Linear scale = 100 μm, n = 8). (C) Safranin O/Fast green staining and (D) OARSI scoring and analysis of cartilage degeneration (n = 10). (E) H&E staining results (Linear scale = 200 μm). (F) IHC results and (G) Aggrecan, COL2A1, MMP13, and COX2, ADAMTS5, iNOS-positive chondrocytes analysis (Linear scale = 100 μm, n = 10). (H) 3D reconstruction and (I)

the tibial plateau transverse sectional images, with white/black arrows indicating osteophytes. (J) H&E images for synovium and (K) Quantitation of maximum osteophyte outgrowth (Linear scale = 1 mm, n = 10). (L) the quantitative analysis of synovitis scores, the black arrow indicates synovial lining cells (Linear scale = 200 μm, n = 10). Data are mean ± SEM. p values are from two-tailed unpaired t-test (B), the Kruskal-Wallis test followed by Dunn's post hoc test (D, L), and the one-way ANOVA test followed by Tukey's post hoc test (G, K).

TRPM2 is essential for chondrocyte damage

To explore the functional role of TRPM2 in the articular chondrocytes, we isolated the primary chondrocytes from WT and *Trpm2*$^{-/-}$ mice and subjected the chondrocytes to IL-1β stimulation. We found that *Trpm2* deficiency significantly attenuated chondrocyte damage, as evidenced by decreased expression of catabolism and inflammation markers (*Mmp13*, *Mmp3*, *iNOS*, and *Cox2*) and elevated expression of an anabolism marker (*Col2a1, Aggrecan*) following IL-1β treatment (Fig. 4A). To further confirm these findings, we performed gain-and loss-of-function assays in primary chondrocytes. the expression of TRPM2 was efficiently silenced or overexpressed by the transfection of *Trpm2* siRNA or *Trpm2*-plasmid (Supplementary Figure. 1B-D). Of note, both RT-qPCR and Western blot analyses demonstrated that chondrocyte inflammation and ECM catabolism were alleviated in *Trpm2* siRNA-transfected chondrocytes exposed to IL-1β treatment (Fig. 4B-F). additionally, the knockdown of *Trpm2* repressed chondrocyte apoptosis following IL-1β induction, as evidenced by reduced protein levels of apoptotic markers (cleaved-Caspase3 and P53) (Fig. 4G, H), and (Bcl-2, Bax, Cyt C) (Supplementary Fig. 3A-B). IF staining also detected similar results in chondrocytes (Fig. 4I-L). Furthermore, we estimated the impact of TRPM2 overexpression on chondrocytes and found that the overexpression of TRPM2 increased mRNA levels of biomarkers associated with chondrocyte catabolism and inflammation in IL-1β-induced chondrocytes (Fig. 4M and Supplementary Fig. 1E-F). These data demonstrate that TRPM2 is essential for the damage of articular chondrocytes.

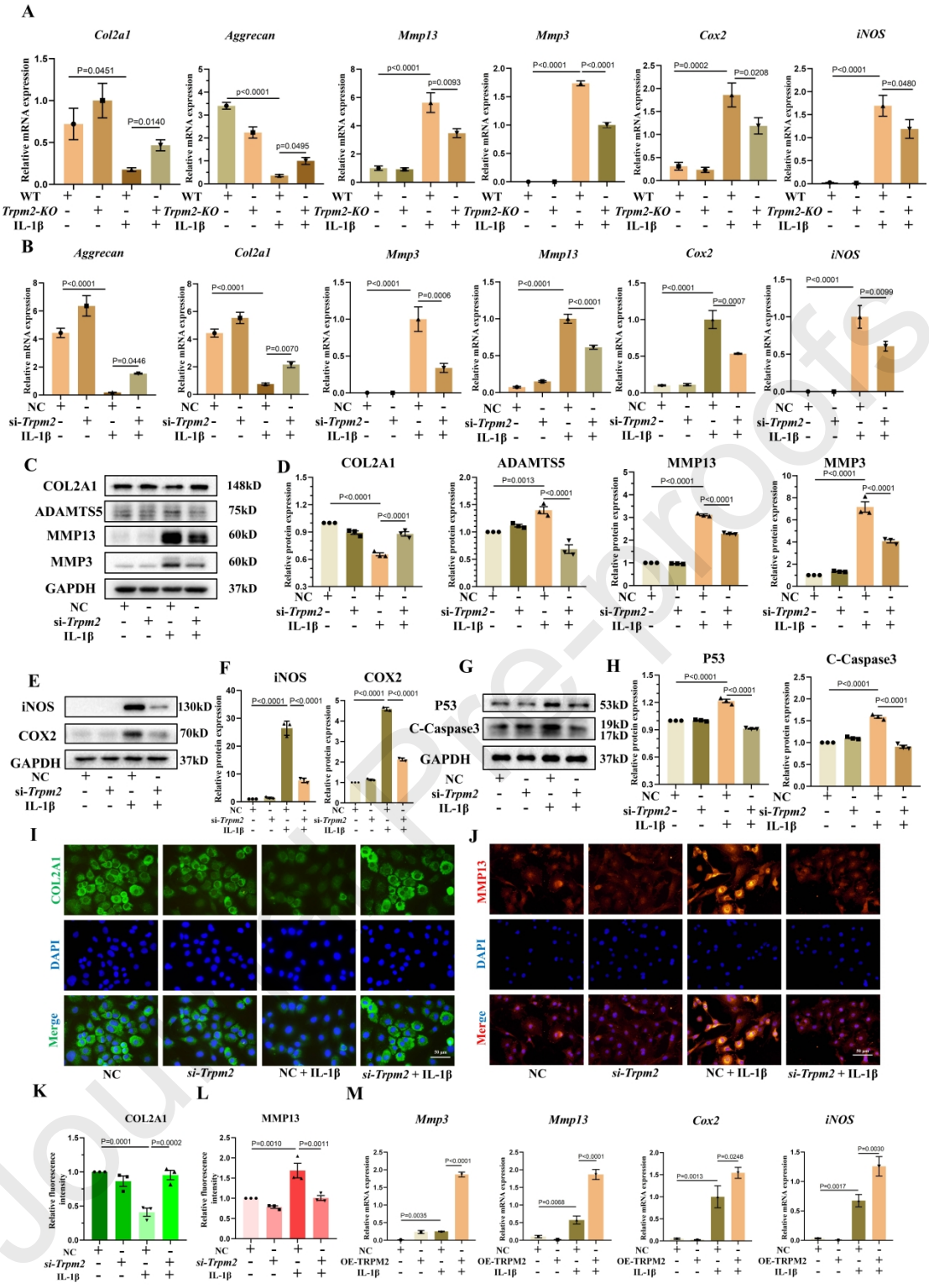

Figure 4 TRPM2 is essential for chondrocyte damage. (A) After the IL-1β treatment for 24 h, the mRNA expression of *Col2a1*, *Aggrecan*, *Mmp13*, *Mmp3*, *Cox2*, and *iNOS* in TRPM2-KO and WT chondrocytes was measured by RT-qPCR. (B) After the siRNA (48 h) and IL-1β (12 h) treatment, the mRNA expression of *Aggrecan*, *Col2a1*, *Mmp13* *Mmp3, Cox2,* and *iNOS,* in primary chondrocytes was measured by RT-qPCR. (C) After the siRNA (48 h) and IL-1β (12 h) treatment, the Western blot results of COL2A1, ADAMTS5, MMP13, and MMP3 and (D) the semiquantitative expression analysis. (E)

The WB results of iNOS, COX2, and (F) semiquantitative expression analysis. (G) The WB results of P53 and cleaved-Caspase3 expression and (H) semiquantitative expression analysis. (I, J) IF images of COL2A1 and MMP13. (K, L) The fluorescence intensity analysis. (M) Chondrocytes were pretreated with overexpression-NC plasmid or overexpression-TRPM2 plasmid for 48 h, followed by IL-1β treatment for 12 h, and the mRNA expression of *Mmp3*, *Mmp13*, *Cox2*, and *iNOS*. Data are mean ± SEM. p values are from a one-way ANOVA test followed by Tukey's post hoc test (A, B, D, F, H, K, L, M).

TRPM2 is upregulated in an NF-κB signaling-dependent manner

As demonstrated in the preceding results, the expression of TRPM2 was observed to be upregulated in OA chondrocytes. To further investigate the potential mechanism behind this, we employed three databases (the UCSC Genome Browser database, Signaling Pathways Project (SPP)-ominer database, and Cistrome Toolkit Data Browser) to predict the potential transcription factors (TFs) of *Trpm2* (Fig. 5A). Given the well-established role of NF-κB in IL-1β-mediated cellular processes and OA pathogenesis[24], We identified RELA (NF-κB-p65) as a promising transcription factor among the candidates. Additionally, we utilized several inhibitors of classical signaling pathways, which are largely associated with OA pathogenesis[18,25-27] (QNZ for NF-Kb signal, LY294002 for PI3K-AKT signal, SP600125 for MAPK-JNK signal, and N-Acetyl-l-cysteine (NAC) for reactive oxygen species signal) to screen for possible TFs. Notably, only the NF-κB inhibitor, QNZ, was able to markedly reverse the upregulation of TRPM2 induced by IL-1β at both the mRNA and protein levels (Fig. 5B, C), indicating a potential role for NF-κB in mediating the transcription of *Trpm2*. Furthermore, the JASPAR database was utilized to predict a potential binding motif, GGGAATTGTC, which was then validated through a ChIP-PCR (Fig. 5D-F). The results demonstrated that RELA can bind to the *Trpm2* promoter at the predicted binding site 2 (344 bp to 335 bp from the upstream of the transcriptional start site) (Fig. 5D–F). The coimmunostaining for TRPM2 and p-P65 in articular cartilage from OA mice revealed a greater degree of colocalization between TRPM2 and p-P65 in OA cartilage compared to normal cartilage (Fig. 5G, H). These findings indicated that p-P65 may be an upstream regulator of TRPM2. To validate this hypothesis, chondrocytes were treated with QNZ, a classic inhibitor of NF-κB. As anticipated, the inhibition of NF-κB activation with QNZ resulted in a suppression of TRPM2, MMP13, and COX2 expression, while reinstating the expression of COL2A1 (Fig. 5I, J). Interestingly, the overexpression of TRPM2 completely reversed the protective effects caused by QNZ treatment (Fig. 5K-N and Supplementary Fig. 5A-B). These data collectively indicate that TRPM2 is upregulated in an NF-κB signaling-dependent manner.

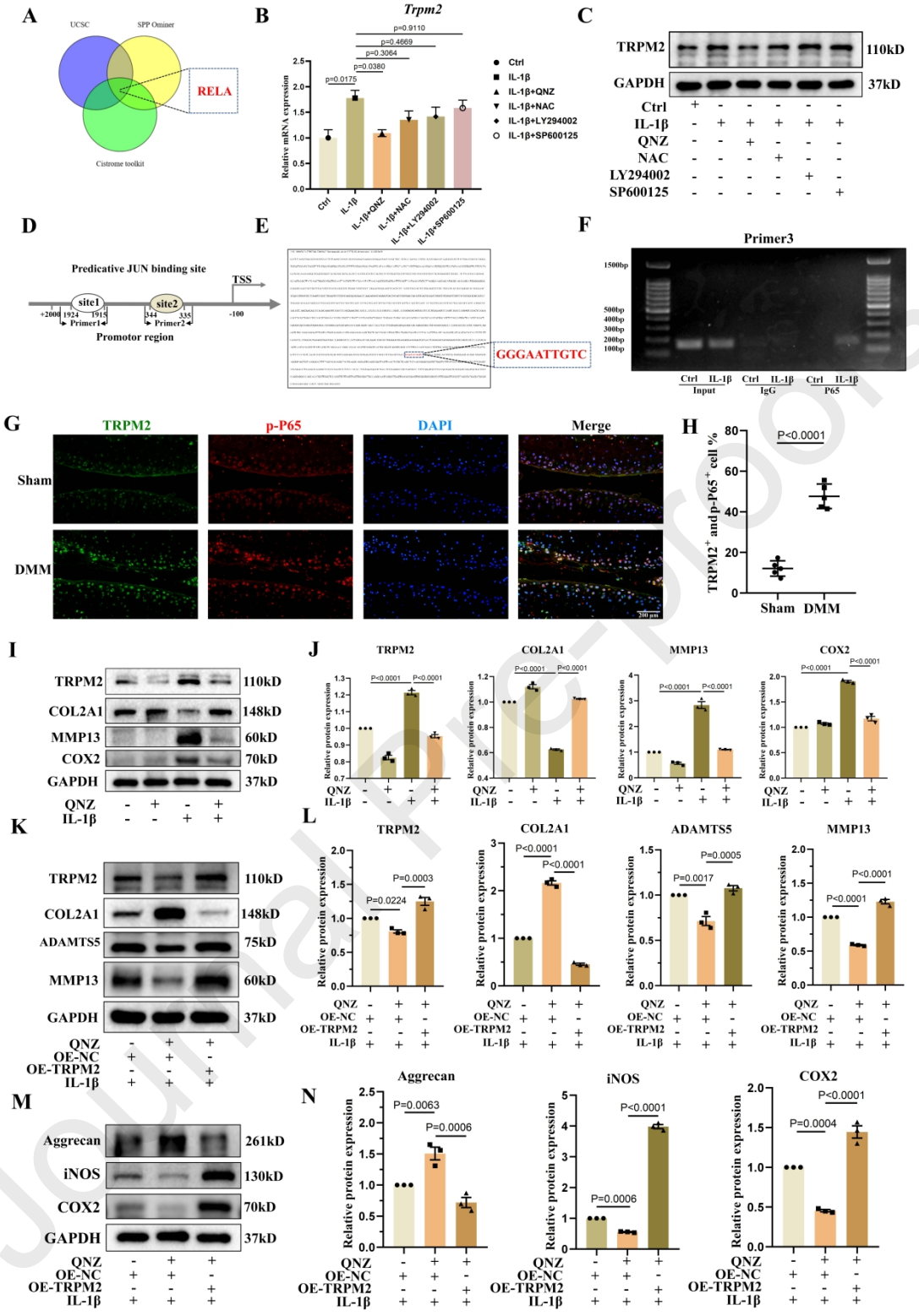

Figure 5 The regulatory mechanism for TRPM2 expression. (A) Transcription factor, RELA (P65), the UCSC Genome Browser database, Signaling Pathways Project (SPP)-ominer database, and Cistrome Toolkit Data Browser were used to screen out. Chondrocytes were treated with IL-1β (24 h) and several signaling pathway inhibitors: QNZ (10 μM), SP600125 (10 μM), NAC (100 μM), and LY294002 (10 μM). (B) The mRNA expression of *Trpm2* in chondrocytes. (C) The WB results of TRPM2 in chondrocytes treated with signaling pathway inhibitors and IL-1β (24 h) are presented

below. (D) The schematic of the predictive binding site of RELA at the promoter. (E) The predicative binding motif of P65 in the promoter of *Trpm2* by using the JASPAR database. (F) ChIP assay results. (G) Coimmunostaining for TRPM2 and p-P65 in articular cartilage. (H) Colocalization ratio analysis between the sham and DMM group (Linear scale = 200 μm). (I) Chondrocytes were treated with QNZ for 1 h and IL-1β treatment for 24 h. WB results of TRPM2, COL2A1, COX2, and MMP13 and (J) quantitative analysis. (K, L) Chondrocytes were treated with TRPM2 overexpression or negative control plasmid for 48 h followed by QNZ and IL-1β treatment for 24 h. The WB results of TRPM2, COL2A1, ADAMTS5, MMP13, and the quantitative expression analysis. (M, N) The WB results of Aggrecan, COX2, iNOS, and the quantitative expression analysis. The data are presented as mean ± SEM. The p values were derived from a one-way ANOVA test followed by Tukey's post hoc test (B, J, L, N) and a two-tailed unpaired t-test (H).

TRPM2 mediates IL-1β-induced intracellular Ca^{2+} influx and initiates mtDNA-cGAS-STING-NF-κB loop

Given that TRPM2 acts as a Ca^{2+}-permeable channel[9], we further investigated whether IL-1β could cause Ca^{2+} influx and Ca^{2+} mediated the effects of TRPM2. We observed that IL-1β treatment increased intracellular Ca^{2+} concentration (Fig. 6A, B). To assess the impact of excessive Ca^{2+} on chondrocytes, we used calcium chloride ($CaCl_2$) to mimic the calcium overload environment *in vitro*. $CaCl_2$ treatment also increased the intracellular concentration of Ca^{2+} and caused ECM degradation (Fig. 6C, D and Supplementary Figure. 4A). Interestingly, knockdown of TRPM2 attenuated the IL-1β or $CaCl_2$-induced Ca^{2+} influx and damage in chondrocytes (Fig. 6A-G).

Cellular Ca^{2+} has a significant role in maintaining mitochondrial function[28]. Mitochondrial DNA (mtDNA) release is one of the manifestations of impaired mitochondrial function and could provoke inflammation via the cGAS-STING pathway[29,30]. Our findings indicate that both IL-1β and Ca^{2+} can stimulate the cGAS-STING pathway, releasing mtDNA (Fig. 6F-G and Supplementary Figure. 4B, C, Supplementary Figure. 6A-C). Furthermore, stimulation of IL-1β resulted in a collapse of the mitochondrial membrane potential and an increase in mitochondrial ROS, as evidenced by JC-1 staining and MitoSOX Red dye staining (Fig. 6H-I). The results indicate that the mtDNA-cGAS-STING axis may be involved in the detrimental effects of excessive Ca^{2+} in chondrocytes. TRPM2- knockdown could alleviate IL-1β or CaCl2-induced mitochondrial membrane potential collapse, increase mitochondrial ROS, and increase cGAS-STING pathway upregulation (Fig. 6F-G). To confirm the role of the mtDNA-cGAS-STING axis in chondrocyte damage, we treated chondrocytes with Cyclosporin A (CsA) (mtDNA inhibitor), RU.521 (cGAS inhibitor), and H-151(STING inhibitor). It was observed that these inhibitors attenuated the activation of the cGAS-STING pathway and improved the metabolism of chondrocytes (Fig. 6J, K, N). Moreover, our results are consistent with previous observations[31,32].

Recent studies have indicated that NF-κB serves as a downstream effector of STING and participates in the STING-mediated inflammatory response[33]. This finding prompted us to investigate the existence of a positive feedback loop involving TRPM2-

Ca^{2+}-cGAS-STING-NF-κB in OA chondrocytes. Notably, TRPM2- knockdown could repress NF-κB pathway activation, and inhibiting mtDNA-cGAS-STING axis had similar inhibitory effects on the NF-κB pathway (Fig. 6M, P, O). This indicates that the TRPM2-Ca^{2+}-cGAS-STING axis is essential for the activation of NF-κB. Since NF-κB acted as an upstream TF for *Trpm2*, these data support the notion that the TRPM2-calcium-cGAS-STING-NF-κB axis forms a pathological feedback loop in chondrocytes.

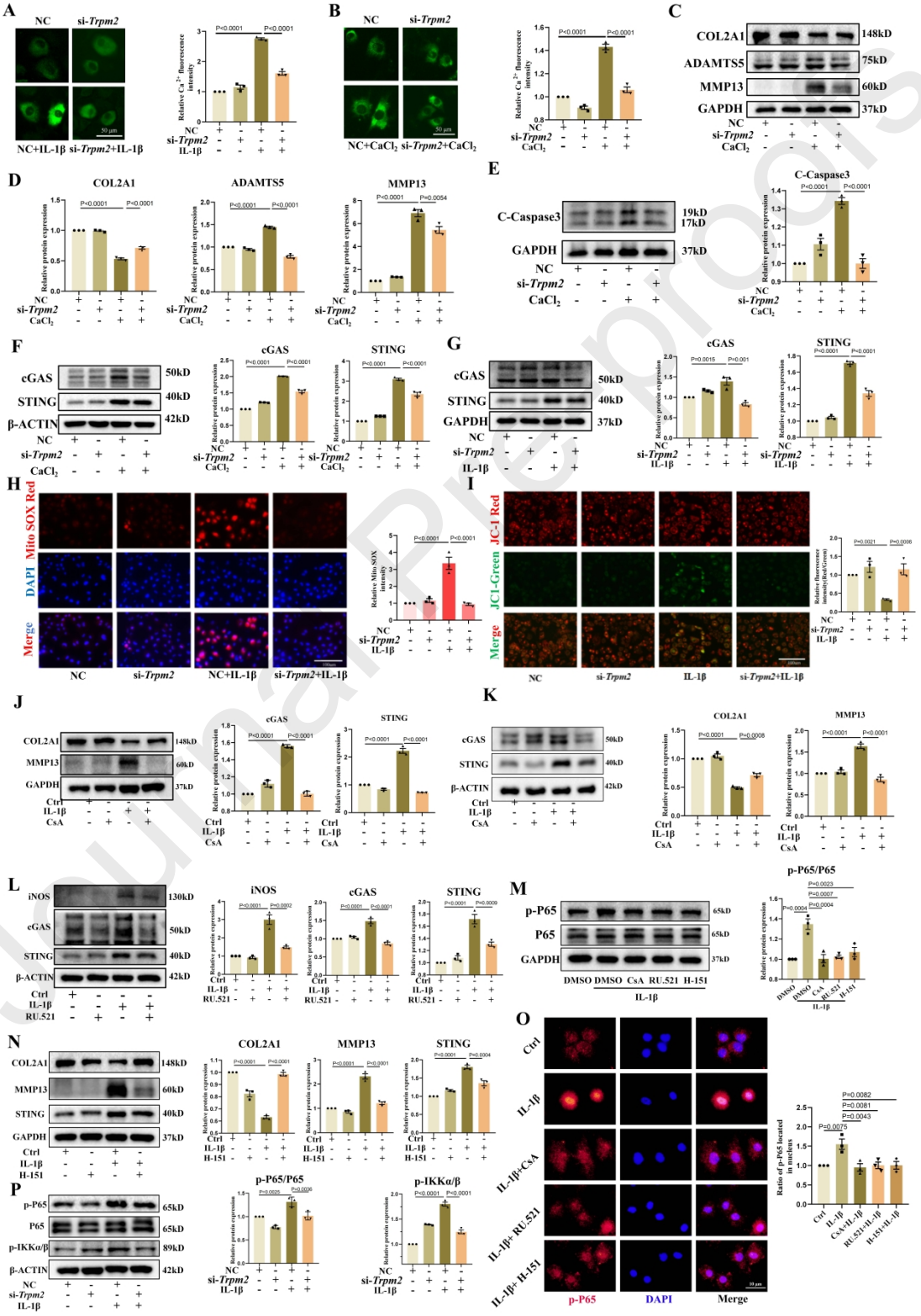

Figure 6 TRPM2 mediates IL-1β-induced intracellular Ca^{2+} influx and initiates mtDNA-cGAS-STING-NF-κB loop. (A, B) Fluo-4 AM staining of Ca^{2+} in chondrocytes and quantitative analysis of intracellular Ca^{2+} levels. (C, D, E) After the siRNA and $CaCl_2$ treatment, the Western blot results of the COL2A1, ADAMTS5, MMP13, Clevaed-Caspase3, and quantitative expression analysis. (F, G) After the siRNA and $CaCl_2$, IL-1β treatment, the Western blot results of the cGAS, STING, and quantitative expression analysis. (H) Examination of mitochondrial ROS by Mito SOX Red and the fluorescence intensity analysis. (I) JC-1 staining results and the fluorescence intensity analysis (Red/Green ratio). (Linear scale = 100 μm). (J, K, L, M, N) After the CsA, H151, RU.521, and IL-1β treatment, WB results of COL2A1, MMP13, iNOS, cGAS, STING, and quantitative expression analysis. (O) IF staining of p-P65. (P) After the siRNA and IL-1β treatment, the Western blot results of the p-P65, P65, and p-IKKα/β, and quantitative expression analysis. Data are mean ± SEM. The p values were derived from a one-way ANOVA test followed by Tukey's post hoc test.

Chelation Ca^{2+} with BAPTA-AM attenuated chondrocyte damage

Considering the central role of Ca^{2+} in TRPM2-mediated chondrocyte damage, it is hypothesized that chelation of Ca^{2+} may have a beneficial effect on reducing chondrocyte damage. BAPTA-AM (a Ca^{2+} chelator) was evaluated in vitro to investigate this possibility. The molecular weight and chemical structure of BAPTA-AM (Fig. 7A). The results demonstrated that at the concentration range of 1-10 μM, BAPTA-AM exhibited no toxicity on chondrocyte viability (Fig. 7B) and BAPTA-AM could significantly reduce $CaCl_2$-induced Ca^{2+} accumulation in chondrocytes (Fig. 7C, D). In addition, Safranin staining and toluene blue staining showed that BAPTA-AM treatment did not change the morphology of chondrocytes. At the same time, it could ameliorate the morphological changes of chondrocytes induced by IL-1β or $CaCl_2$ (Fig. 7E). It was also found that BAPT-AM treatment improved IL-1β or $CaCl_2$-related damage in chondrocytes, as evidenced by restoration of chondrocyte proliferation (EdU staining) (Fig. 7F-G) and reduction of inflammation (iNOS and COX2 expression), apoptosis (P53 and Cleaved-Caspase3 expression), and impaired ECM metabolism (COL2A1, MMP3, and MMP13 expression) (Fig. 7H-M). Collectively, these data suggest that BAPT-AM could protect against chondrocyte damage.

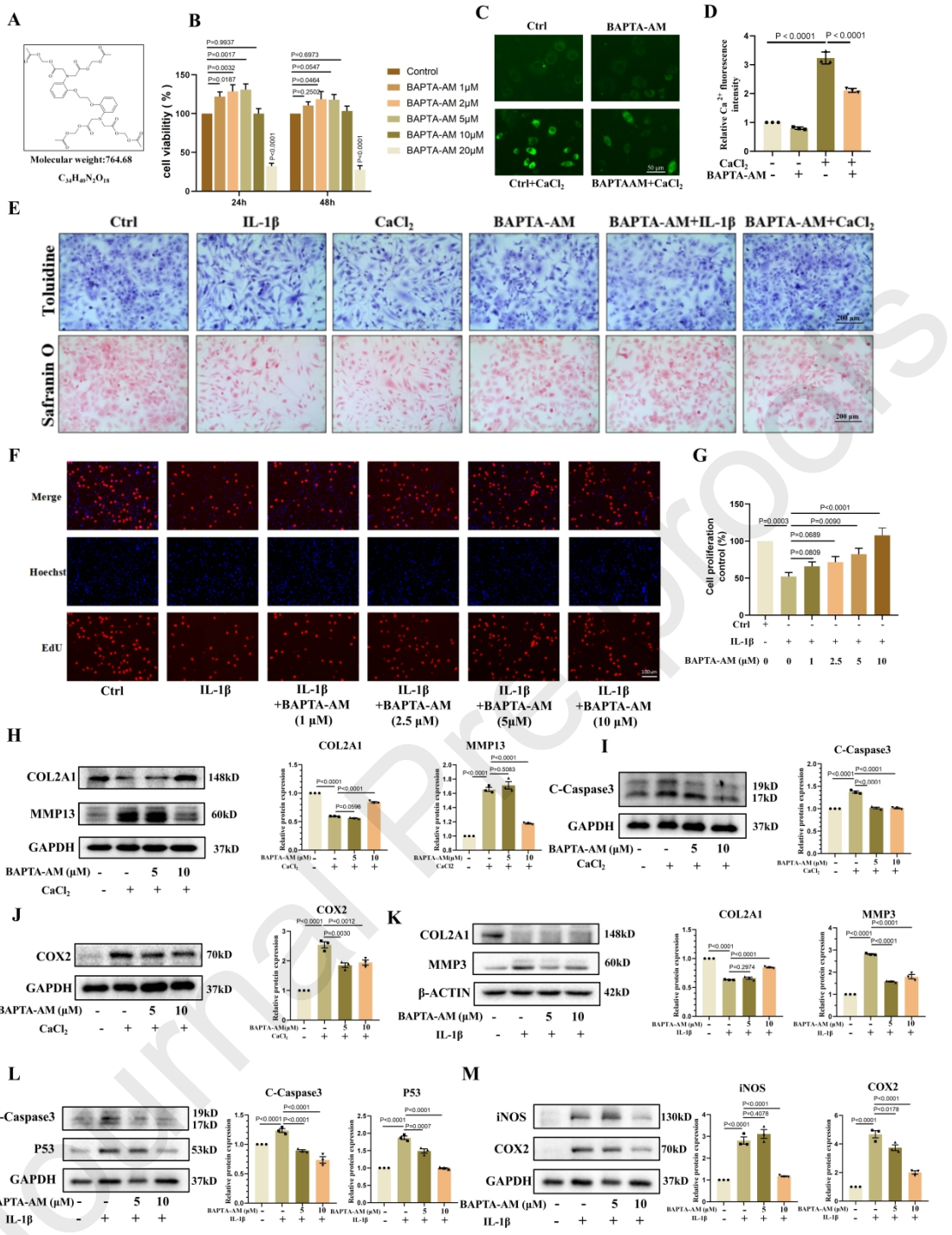

Figure 7 The effects of BAPTA-AM on chondrocytes. (A) BAPTA-AM chemical structure and molecular weight. (B) Chondrocyte toxicity of BAPTA-AM at different concentrations detected by CCK8. (C) Chondrocytes were treated with BAPTA-AM (5 μM) and $CaCl_2$ (5 μM). Representative fluorescence imaging of intracellular Ca^{2+} measured by Fluo-4 AM (Linear scale = 50 μm) and (D) Fluorescence intensity analysis. (E) Chondrocytes were treated with BAPTA-AM, IL-1β or $CaCl_2$. Toluidine blue and Safranin O staining (Linear scale = 200 μm). (F) BAPTA-AM treatment at different concentrations. Proliferating chondrocytes were positively stained by EdU (Linear scale =100 μm). (G) EdU-positive chondrocytes analysis. Chondrocytes were treated

with BAPTA-AM and $CaCl_2$. (H, I, J) WB results of COL2A1, MMP13, cleaved-Caspase3, and COX2 quantitative analysis of the expression. (K, L, M) After the BAPTA-AM and IL-1β treatment, the WB results of COL2A1, MMP13, Cleaved Caspase3, P53 iNOS, and COX2 quantitative analysis of the expression. Data are mean ± SEM. The p-values were derived from two-tailed unpaired t-tests (B, G) and one-way ANOVA tests, which were then subjected to Tukey's post hoc tests (D, H, I, K, M).

Administration of BAPTA-AM attenuated DMM-induced OA

Based on the findings above, we sought to validate whether calcium chelation with BAPTA-AM could protect against OA progression. Different doses of BAPTA-AM (1.5 μg/kg and 15 μg/kg) were intra-articularly injected to achieve local administration. One week after DMM surgery, BAPTA-AM or vehicle control was administered once a week for a continuous period of 8 weeks. As depicted in Fig. 8A-C, strikingly attenuated cartilage degeneration was detected in BAPTA-AM treated mice, as shown by the safranin O/Fast and H&E staining and validated by a lower OARSI score and increased cartilage thickness (Supplementary Figure. 5C) compared to the DMM mice. Consistently, mice administered BAPTA-AM exhibited significant attenuation of catabolism marker (MMP13, ADAMTS5) and inflammation marker (COX2, iNOS) and improvement of anabolism markers (COL2A1 and Aggrecan) compared with the DMM group (Fig. 8H, I). Additionally, the severity of osteophyte formation and synovitis were reduced by BAPTA-AM treatment (Fig. 8D-G). Collectively, these results demonstrate the therapeutic effects of BAPTA-AM on DMM-induced OA.

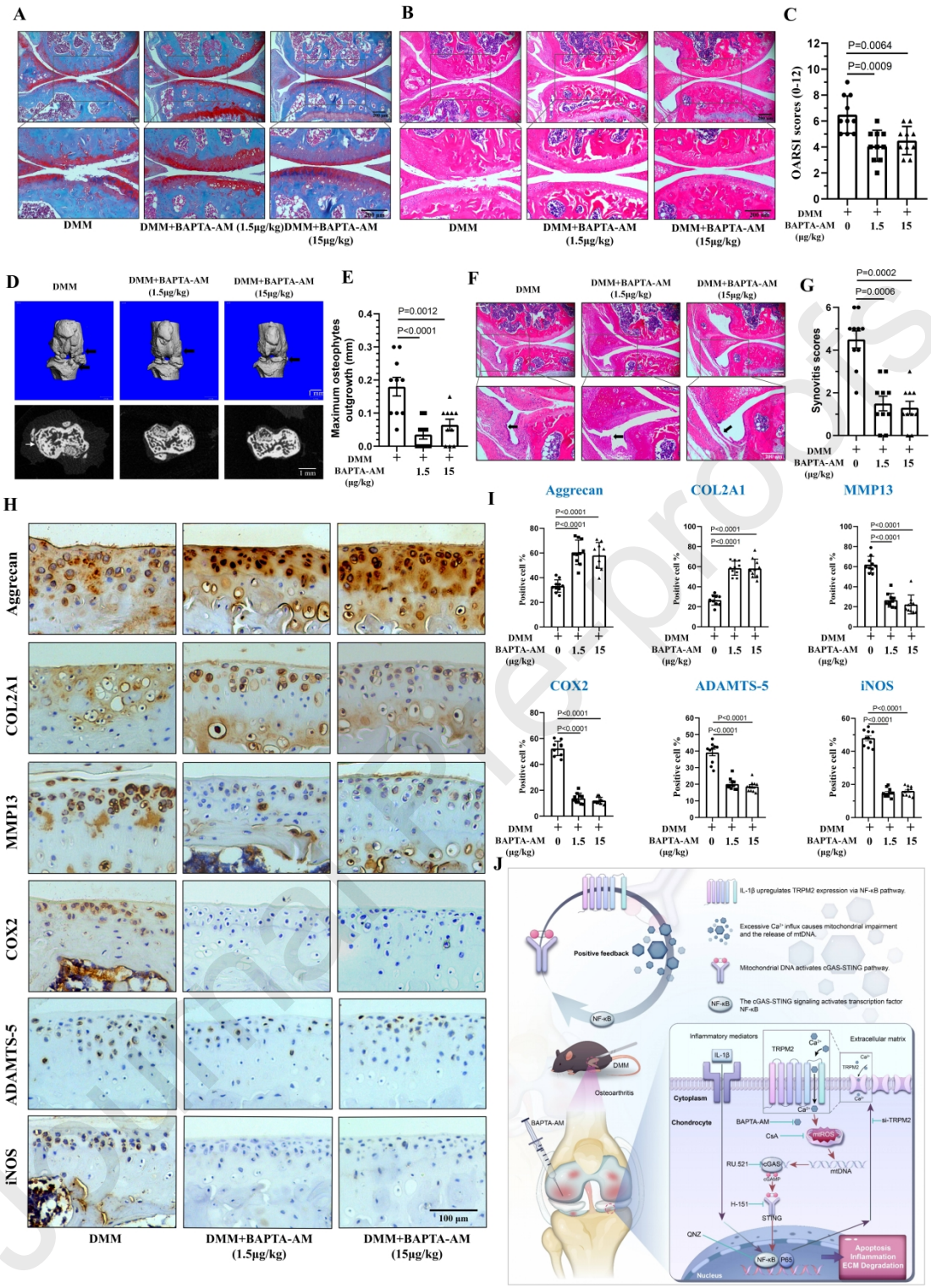

Figure 8 BAPTA-AM administration alleviated DMM-induced OA. The mice were divided into DMM, DMM + BAPTA-AM (1.5 μg/kg), and DMM + BAPTA-AM (15 μg/kg) groups. After a week of DMM surgery, 10 μl of BAPTA-AM solution or PBS was intra-articularly injected weekly. Images of Safranin O/Fast green staining (A) and (B) H&E staining (Linear scale = 200 μm). (C) The OARSI scores analysis for cartilage degeneration (n = 10). (D) 3D reconstruction images and the tibial plateau transverse sectional images (Linear scale = 1 mm). (E) Quantitation of maximum osteophyte

outgrowth (n = 10). (F) H&E staining of synovium and (G) the quantitative analysis of synovitis scores, the black arrow indicates synovial lining cells (Linear scale = 200 μm, n = 10). (H) IHC images (Linear scale = 100 μm) and (I) quantitative analysis of Aggrecan, COL2A1, MMP13, COX2, ADAMTS5, and iNOS (n = 10). (J) The graphic illustration of this study. Data are mean ± SEM. p values are from the Kruskal-Wallis test followed by Dunn's post hoc test (C, I), and the one-way ANOVA test followed by Tukey's post hoc test (E, G).

Discussion

The chondrocyte is the sole cell type within articular cartilage, which is crucial in maintaining cartilage homeostasis. When chondrocytes are damaged, they significantly contribute to the progression of OA[34,35]. Consequently, it is essential to identify the mechanisms that greatly influence the fate and function of chondrocytes. Our study illustrates that TRPM2 acts as a bridge between inflammatory mediators and calcium homeostasis in chondrocytes. Recent research has reported that HIF-1α promoted TRPM2 gene expression via transcriptional regulation in TG neurons[36]. NF-κB plays a critical role in OA pathology[37]. Our results indicated that IL-1β upregulates TRPM2 in an NF-κB-dependent manner, facilitating TRPM2-mediated calcium influx. Excessive intracellular calcium leads to mitochondrial dysfunction and the release of mtDNA, which activates the cGAS-STING-NF-κB signaling pathway, culminating in a positive feedback loop. This cascade ultimately results in chondrocyte damage and cartilage degeneration. Therefore, targeting the TRPM2-calcium axis may offer a novel therapeutic avenue for OA (see Fig. 8J).

Calcium ions are indispensable in various cellular physiological processes. However, unregulated accumulation of calcium can lead to several pathological conditions, including oxidative stress, apoptosis, and inflammation[38-40]. Numerous studies have implicated excess intracellular Ca2+ in promoting chondrocyte damage associated with OA development[7,41,42]. Our findings corroborate these prior investigations by demonstrating that TRPM2 serves as a calcium influx channel in chondrocytes, with its upregulation contributing to chondrocyte dysfunction and apoptosis. Notably, PIEZO1 functions as a mechanosensitive channel, while TRPM2 is sensitive to oxidative stress[43,44]. Both mechanical and oxidative stress are recognized pathological factors in OA[45,46], underscoring the critical roles of TRPM2 and PIEZO1 in OA pathogenesis.

Excessive calcium ions can act as pathological mediators, triggering multiple signaling pathways and harmful processes [5]. One noteworthy example is activating the mtDNA-cGAS-STING pathway by calcium ions, which can induce inflammation and innate immunity[29,30]. Additionally, calcium ions can lead to mitochondrial dysfunction and subsequent mitochondria-related apoptosis[47]. Our study confirmed that calcium ions can cause mitochondrial dysfunction and mtDNA release in chondrocytes, activating the cGAS-STING-NF-κB pathway. Importantly, separately inhibiting TRPM2, Ca^{2+}, or the cGAS-STING-NF-κB pathway can ameliorate these detrimental effects. These results suggest the existence of a TRPM2-mediated pathological positive feedback loop,

whereby inflammatory mediators induce increased expression of TRPM2 via the NF-κB signaling pathway. The subsequent upregulation of TRPM2 facilitates calcium influx and activates the cGAS-STING-NF-κB signaling pathway, ultimately exacerbating chondrocyte damage. TRPM2 has been reported in neurological diseases[48], inflammatory diseases[49], cardiovascular diseases[50], and cancer[51]. The TRPM2-Ca^{2+}-cGAS-STING-NF-κB signaling axis may represent a novel pathological mechanism for investigating these diseases.

In light of these findings, targeting the TRPM2-Ca^{2+} axis presents a promising therapeutic strategy for OA. However, a selective inhibitor for TRPM2 is currently lacking. In our investigation, we have preliminarily demonstrated the protective effects of calcium chelation using BAPTA-AM in the DMM murine model. This represents an initial step toward clinical application, and future studies should assess the efficacy and safety of BAPTA-AM in larger animal models. Given the role of TRPM2 in various inflammatory and degenerative diseases, including OA, there is a compelling need to develop more selective inhibitors targeting TRPM2.

Conclusions

In summary, this study elucidates the dysregulation of TRPM2 during OA. Our findings indicate that TRPM2 plays a significant role in the pathogenesis of OA in murine models, with TRPM2 knockout contributing to a delay in OA progression. Furthermore, we identified a TRPM2-mediated pathological feed-forward loop in chondrocytes, mediated through the Ca^{2+}-cGAS-STING-NF-κB signaling axis. Based on these findings, the inhibition of the TRPM2-Ca^{2+} axis with BAPTA-AM may offer a novel therapeutic strategy for OA.

Ethics statement

The collection of human cartilage was approved by the Ethics Committee of Tongji Hospital (TJ-IRB20210905) after obtaining informed consent from the patients. The animal experiment was approved by the Ethics Committee of Tongji Hospital (TJH-202212051).

Acknowledgments

This study was supported by the National Natural Science Foundation of China (no. 82302768; 82172498; 11602155), Special Fund for Knowledge Innovation of Wuhan Science and Technology Bureau (no.2022020801010557), Health Commission of Hubei Province Scientific Research Project (no. WJ2021Q002), and Hubei Provincial Natural Science Foundation (no.2021CFB529).

Conflicts of interest

There are no conflicts of interest.

References

1. Hunter DJ, Bierma-Zeinstra S. Osteoarthritis. *Lancet* 2019;**393**:1745-59.

2. Hodgkinson T, Kelly DC, Curtin CM, O Brien FJ. Mechanosignalling in cartilage: An emerging target for the treatment of osteoarthritis. *Nat Rev Rheumatol* 2022;**18**:67-84.

3. Zheng L, Zhang Z, Sheng P, Mobasheri A. The role of metabolism in chondrocyte dysfunction and the progression of osteoarthritis. *Ageing Res Rev* 2021;**66**:101249.

4. Giorgi C, Marchi S, Pinton P. The machineries, regulation and cellular functions of mitochondrial calcium. *Nat Rev Mol Cell Bio* 2018;**19**:713-30.

5. Bagur R, Hajnóczky G. Intracellular Ca^{2+} Sensing: Its Role in Calcium Homeostasis and Signaling. *Mol Cell* 2017;**66**:780-8.

6. Montes De Oca Balderas P. Mitochondria–plasma membrane interactions and communication. *J Biol Chem* 2021;**297**.

7. Lee W, Nims RJ, Savadipour A, Zhang Q, Leddy HA, Liu F, et al. Inflammatory signaling sensitizes Piezo1 mechanotransduction in articular chondrocytes as a pathogenic feed-forward mechanism in osteoarthritis. *Proceedings of the National Academy of Sciences* 2021;**118**:e2001611118.

8. Agarwal P, Lee H, Smeriglio P, Grandi F, Goodman S, Chaudhuri O, et al. A dysfunctional TRPV4–GSK3β pathway prevents osteoarthritic chondrocytes from sensing changes in extracellular matrix viscoelasticity. *Nat Biomed Eng* 2021;**5**:1472-84.

9. Huang Y, Winkler PA, Sun W, Lü W, Du J. Architecture of the TRPM2 channel and its activation mechanism by ADP-ribose and calcium. *Nature* 2018;**562**:145-9.

10. Wang L, Fu T, Zhou Y, Xia S, Greka A, Wu H. Structures and gating mechanism of human TRPM2. *Science* 2018;**362**:v4809.

11. Park L, Wang G, Moore J, Girouard H, Zhou P, Anrather J, et al. The key role of transient receptor potential melastatin-2 channels in amyloid-β-induced

neurovascular dysfunction. *Nat Commun* 2014;**5**:5318.

12. Hermosura MC, Cui AM, Go RCV, Davenport B, Shetler CM, Heizer JW, et al. Altered functional properties of a TRPM2 variant in Guamanian ALS and PD. *Proceedings of the National Academy of Sciences* 2008;**105**:18029-34.

13. Alves-Lopes R, Neves KB, Anagnostopoulou A, Rios FJ, Lacchini S, Montezano AC, et al. Crosstalk between vascular redox and calcium signaling in hypertension involves TRPM2 (Transient receptor potential melastatin 2) cation channel. *Hypertension* 2020;**75**:139-49.

14. Wang H, David AY, Andrew DR, Xin X, Tim EC, Carole JP. Oxidative changes and signalling pathways are pivotal in initiating age-related changes in articular cartilage. *Ann Rheum Dis* 2016;**75**:449.

15. West AP, Khoury-Hanold W, Staron M, Tal MC, Pineda CM, Lang SM, et al. Mitochondrial DNA stress primes the antiviral innate immune response. *Nature* 2015;**520**:553-7.

16. Liu H, Chi R, Xu J, Guo J, Guo Z, Zhang X, et al. DMT1-mediated iron overload accelerates cartilage degeneration in Hemophilic Arthropathy through the mtDNA-cGAS-STING axis. *Biochim Biophys Acta Mol Basis Dis* 2024;**1870**:167058.

17. Liang S, Wang ZG, Zhang ZZ, Chen K, Lv ZT, Wang YT, et al. Decreased RIPK1 expression in chondrocytes alleviates osteoarthritis via the TRIF/MyD88-RIPK1-TRAF2 negative feedback loop. *Aging (Albany NY)* 2019;**11**:8664-80.

18. Sun K, Hou L, Guo Z, Wang G, Guo J, Xu J, et al. JNK-JUN-NCOA4 axis contributes to chondrocyte ferroptosis and aggravates osteoarthritis via ferritinophagy. *Free Radical Bio Med* 2023.

19. Rowe MA, Harper LR, Mcnulty MA, Lau AG, Carlson CS, Leng L, et al. Reduced osteoarthritis severity in aged mice with deletion of macrophage migration inhibitory factor. *Arthritis Rheumatol* 2017;**69**:352-61.

20. Lewis JS, Hembree WC, Furman BD, Tippets L, Cattel D, Huebner JL, et al. Acute joint pathology and synovial inflammation is associated with increased intra-articular fracture severity in the mouse knee. *Osteoarthr Cartilage* 2011;**19**:864-73.

21. Hou L, Wang G, Zhang X, Lu F, Xu J, Guo Z, et al. Mitoquinone alleviates osteoarthritis progress by activating the NRF2-Parkin axis. *iScience* 2023;**26**.

22. Roelofs AJ, Kania K, Rafipay AJ, Sambale M, Kuwahara ST, Collins FL, et al. Identification of the skeletal progenitor cells forming osteophytes in

osteoarthritis. *Ann Rheum Dis* 2020;**79**:1625-34.

23. Sanchez-Lopez E, Coras R, Torres A, Lane NE, Guma M. Synovial inflammation in osteoarthritis progression. *Nat Rev Rheumatol* 2022;**18**:258-75.

24. Lepetsos P, Papavassiliou KA, Papavassiliou AG. Redox and NF-κB signaling in osteoarthritis. *Free Radical Bio Med* 2019;**132**:90-100.

25. Arra M, Swarnkar G, Ke K, Otero JE, Ying J, Duan X, et al. LDHA-mediated ROS generation in chondrocytes is a potential therapeutic target for osteoarthritis. *Nat Commun* 2020;**11**:3427.

26. Sun K, Luo J, Guo J, Yao X, Jing X, Guo F. The PI3K/AKT/mTOR signaling pathway in osteoarthritis: A narrative review. *Osteoarthr Cartilage* 2020.

27. Sun K, Luo J, Jing X, Xiang W, Guo J, Yao X, et al. Hyperoside ameliorates the progression of osteoarthritis: An in vitro and in vivo study. *Phytomedicine* 2021;**80**:153387.

28. Madreiter-Sokolowski CT, Thomas C, Ristow M. Interrelation between ROS and Ca2+ in aging and age-related diseases. *Redox Biol* 2020;**36**:101678.

29. Xian H, Watari K, Sanchez-Lopez E, Offenberger J, Onyuru J, Sampath H, et al. Oxidized DNA fragments exit mitochondria via mPTP- and VDAC-dependent channels to activate NLRP3 inflammasome and interferon signaling. *Immunity* 2022;**55**:1370-85.

30. Sabateeshan, Mathavarajah, Jayme, Salsman, Graham, Dellaire. An emerging role for calcium signalling in innate and autoimmunity via the cGAS-STING axis. *Cytokine Growth F R* 2019.

31. Guo Q, Chen X, Chen J, Zheng G, Xie C, Wu H, et al. STING promotes senescence, apoptosis, and extracellular matrix degradation in osteoarthritis via the NF-κB signaling pathway. *Cell Death Dis* 2021;**12**:13.

32. Shin Y, Cho D, Kim SK, Chun JS. STING mediates experimental osteoarthritis and mechanical allodynia in mouse. *Arthritis Res Ther* 2023;**25**:90.

33. Balka KR, Louis C, Saunders TL, Smith AM, Calleja DJ, D Silva DB, et al. TBK1 and IKKε Act Redundantly to Mediate STING-Induced NF-κB Responses in Myeloid Cells. *Cell Rep* 2020;**31**.

34. Fosang AJ, Beier F. Emerging Frontiers in cartilage and chondrocyte biology. *Best Practice & Research Clinical Rheumatology* 2011;**25**:751-66.

35. Stegen S, Rinaldi G, Loopmans S, Stockmans I, Moermans K, Thienpont B, et al. Glutamine metabolism controls chondrocyte identity and function. *Dev Cell*

2020;**53**:530-44.

36. Ma C, Zhu C, Zhang Y, Yu M, Song Y, Chong Y, et al. Gastrodin alleviates NTG-induced migraine-like pain via inhibiting succinate/HIF-1alpha/TRPM2 signaling pathway in trigeminal ganglion. *Phytomedicine* 2024;**125**:155266.

37. Yao Q, Wu X, Tao C, Gong W, Chen M, Qu M, et al. Osteoarthritis: Pathogenic signaling pathways and therapeutic targets. *Signal Transduct Target Ther* 2023;**8**:56.

38. Fan M, Zhang J, Tsai C, Orlando BJ, Rodriguez M, Xu Y, et al. Structure and mechanism of the mitochondrial Ca2+ uniporter holocomplex. *Nature* 2020;**582**:129-33.

39. Luongo TS, Lambert JP, Gross P, Nwokedi M, Lombardi AA, Shanmughapriya S, et al. The mitochondrial Na+/Ca2+ exchanger is essential for Ca2+ homeostasis and viability. *Nature* 2017;**545**:93-7.

40. Calvo-Rodriguez M, Hou SS, Snyder AC, Kharitonova EK, Russ AN, Das S, et al. Increased mitochondrial calcium levels associated with neuronal death in a mouse model of Alzheimer's disease. *Nat Commun* 2020;**11**:2146.

41. Wang S, Li W, Zhang P, Wang Z, Ma X, Liu C, et al. Mechanical overloading induces GPX4-regulated chondrocyte ferroptosis in osteoarthritis via Piezo1 channel facilitated calcium influx. *J Adv Res* 2022;**41**:63-75.

42. Wang Y, Xiang C, Sun X, Wu S, Lv J, Li P, et al. DAla2GIP antagonizes H2O2-induced chondrocyte apoptosis and inflammatory factor secretion. *Bone* 2019;**127**:656-63.

43. Zhao Q, Zhou H, Chi S, Wang Y, Wang J, Geng J, et al. Structure and mechanogating mechanism of the Piezo1 channel. *Nature* 2018;**554**:487-92.

44. Malko P, Jiang L. TRPM2 channel-mediated cell death: An important mechanism linking oxidative stress-inducing pathological factors to associated pathological conditions. *Redox Biol* 2020;**37**:101755.

45. Sun K, Jing X, Guo J, Yao X, Guo F. Mitophagy in degenerative joint diseases. *Autophagy* 2020:1-11.

46. Zhen G, Guo Q, Li Y, Wu C, Zhu S, Wang R, et al. Mechanical stress determines the configuration of TGFβ activation in articular cartilage. *Nat Commun* 2021;**12**:1706.

47. Xue Y, Morris JL, Yang K, Fu Z, Zhu X, Johnson F, et al. SMARCA4/2 loss inhibits chemotherapy-induced apoptosis by restricting IP3R3-mediated Ca2+ flux to mitochondria. *Nat Commun* 2021;**12**:5404.

48. Belrose JC, Jackson MF. TRPM2: A candidate therapeutic target for treating neurological diseases. *Acta Pharmacol Sin* 2018;**39**:722-32.

49. Wang L, Negro R, Wu H. TRPM2, linking oxidative stress and Ca(2+) permeation to NLRP3 inflammasome activation. *Curr Opin Immunol* 2020;**62**:131-5.

50. Malko P, Jiang LH. TRPM2 channel-mediated cell death: An important mechanism linking oxidative stress-inducing pathological factors to associated pathological conditions. *Redox Biol* 2020;**37**:101755.

51. Miller BA. TRPM2 in cancer. *Cell Calcium* 2019;**80**:8-17.